Am J Physiol Cell Physiol
281: C114–C122, 2001.

Deficiency in parvalbumin increases fatigue resistance in fast-twitch muscle and upregulates mitochondria

GAOPING CHEN,[1] STEFANIE CARROLL,[2] PETER RACAY,[3] JIM DICK,[4] DIRK PETTE,[5] IRMTRUD TRAUB,[5] GERTA VRBOVA,[4] PETER EGGLI,[1] MARCO CELIO,[3] AND BEAT SCHWALLER[3]

[1]*Institute of Anatomy, University of Bern, CH-3012 Bern, and* [3]*Program in Neuroscience, Institute of Histology and General Embryology, University of Fribourg, CH-1705 Fribourg, Switzerland;* [2]*National Institutes of Health, Bethesda, Maryland 20814;* [4]*Deptartment of Anatomy, University College, London WC1E 6BT, United Kingdom; and* [5]*Faculty of Biology, University of Constance, D-78457 Constance, Germany*

Received 19 July 2000; accepted in final form 5 February 2001

Chen, Gaoping, Stefanie Carroll, Peter Racay, Jim Dick, Dirk Pette, Irmtrud Traub, Gerta Vrbova, Peter Eggli, Marco Celio, and Beat Schwaller. Deficiency in parvalbumin increases fatigue resistance in fast-twitch muscle and upregulates mitochondria. *Am J Physiol Cell Physiol* 281: C114–C122, 2001.—The soluble Ca^{2+}-binding protein parvalbumin (PV) is expressed at high levels in fast-twitch muscles of mice. Deficiency of PV in knockout mice (PV −/−) slows down the speed of twitch relaxation, while maximum force generated during tetanic contraction is unaltered. We observed that PV-deficient fast-twitch muscles were significantly more resistant to fatigue than were the wild type. Thus components involved in Ca^{2+} homeostasis during the contraction-relaxation cycle were analyzed. No upregulation of another cytosolic Ca^{2+}-binding protein was found. Mitochondria are thought to play a physiological role during muscle relaxation and were thus analyzed. The fractional volume of mitochondria in the fast-twitch muscle extensor digitorum longus (EDL) was almost doubled in PV −/− mice, and this was reflected in an increase of cytochrome *c* oxidase. A faster removal of intracellular Ca^{2+} concentration ($[Ca^{2+}]_i$) 200–700 ms after fast-twitch muscle stimulation observed in PV −/− muscles supports the role for mitochondria in late $[Ca^{2+}]_i$ removal. The present results also show a significant increase of the density of capillaries in EDL muscles of PV −/− mice. Thus alterations in the dynamics of Ca^{2+} transients detected in fast-twitch muscles of PV −/− mice might be linked to the increase in mitochondria volume and capillary density, which contribute to the greater fatigue resistance of these muscles.

muscle fatigue; calcium-binding protein; EF hand; compensation

MOST MAMMALIAN SKELETAL MUSCLES are classified as either fast or slow twitch, depending on the time course of the excitation-contraction-relaxation (ECR) cycle caused by brief neural stimulation. The different phases of this cycle in fibers after propagation of an action potential along the membrane consist of *1*) recognition of the depolarization signal by the T tubule system and transmission of this signal to sarcoplasmic reticulum (SR) membranes, *2*) release of Ca^{2+} from SR resulting in increased intracellular Ca^{2+} concentration ($[Ca^{2+}]_i$) in the myoplasm, *3*) activation of Ca^{2+}-dependant regulatory systems and binding of Ca^{2+} to the contractile machinery (troponin C) resulting in fiber contraction, and *4*) removal of Ca^{2+} by cytoplasmic proteins and reuptake into SR by SR Ca^{2+}-ATPase (muscle relaxation phase). In each of these steps, homologous molecular components (isoforms) are found in the various types of muscle fibers, resulting in differences in the kinetics of the ECR cycle and in the force generated during a twitch. The fatigability of the different muscle fibers is linked to variations in the fiber type-specific components (for a review, see Ref. 34). In addition, not all steps of the ECR cycle display the same sensitivity to fatigue. Various methods have been used to dissect the phases of the ECR cycle and to investigate the roles of fiber-specific components in the ECR cycle and their contribution to fatigue sensitivity or resistance. A marked increase in resistance to fatigue was detected in fast-twitch fibers that were chronically stimulated at low frequency (CLFS) (Ref. 17; for a review, see Ref. 27). During CLFS, several changes at the molecular level occur, including changes in myosin heavy chain (MHC) and troponin isoforms. Increases in mitochondrial volume and enzyme activities of aerobic oxidative metabolism are observed as well as changes in activities of Ca^{2+} release and uptake (7) and also myoplasmic Ca^{2+}-binding sites (14, 16, 26).

Parvalbumin (PV), the main soluble Ca^{2+}-binding protein present only in fast-twitch fibers, is rapidly downregulated after CLFS (16). This protein was demonstrated to act as a relaxation factor in amphibians (18, 37), and, recently, also in mammals in vitro (25)

Address for reprint requests and other correspondence: B. Schwaller, Institute of Histology and General Embryology, Univ. of Fribourg, CH-1705 Fribourg, Switzerland (E-mail: beat.schwaller@unifr.ch).

The costs of publication of this article were defrayed in part by the payment of page charges. The article must therefore be hereby marked "*advertisement*" in accordance with 18 U.S.C. Section 1734 solely to indicate this fact.

and in vivo (31). The recently generated PV knockout mice (PV −/−) (31) represent an independent model to investigate the role of PV during muscle contraction and relaxation. In these mice, it was shown that PV is responsible for the fast initial drop of $[Ca^{2+}]_i$, which helps to considerably shorten the duration of a single-twitch contraction and relaxation. In PV −/− mice, the time-to-peak twitch force, and, in particular, the half-relaxation time, is increased compared with wild-type (WT) mice. In this report, we investigated how fast-twitch muscles cope with the lack of the myoplasmic Ca^{2+} buffer PV, specifically whether PV deficiency is compensated by upregulation of another Ca^{2+} buffer, and how this might affect the fatigability of fast-twitch muscles of PV −/− mice.

MATERIALS AND METHODS

Animals. PV-deficient (PV −/−), heterozygous (PV +/−), or WT (PV +/+) mice generated on a mixed 129/Ola × C57BL/6J genetic background (31) were used in this study. Tail biopsies from all mice were used to genotype animals by PCR, and the genotype of all mice was masked from the experimenters until data had been evaluated.

Muscle contraction. Experiments on the contractile properties of a fast-twitch muscle, the tibialis anterior (TA), were carried out essentially as described previously (31). The distal tendons of the TA muscles of anaesthetized mice (intraperitoneal injection of a 4.5% solution of chloral hydrate; 1 ml/100 g of body wt) were dissected on both sides from the surrounding tissue. They were cut, attached to a silk thread, and the sciatic nerve was dissected. All of its branches, except for the common peroneal nerve, were sectioned. The nerve was cut and its distal stump prepared for stimulation. The lower limbs were secured to a rigid table by pins through the knee and ankle joints. The muscle was then connected by the silk thread to strain gauges. Contractions were elicited by supramaximal stimulation of the distal stump of the sciatic nerve using bipolar silver electrodes. The length of the muscles was adjusted to obtain maximum twitch tension in response to a single stimulus to the nerve. Isometric contractions were displayed on a storage oscilloscope screen, the images photographed, and values of single and tetanic contractions were calculated from these photographs. Muscle fatigue was tested by subjecting the muscles to trains of tetanic contractions at 40 Hz with a 250-ms duration every second for 5 min, displayed on a devices pen recorder. A fatigue index was calculated by dividing the force produced at the end of the 5-min stimulation by that produced by the muscle at the beginning of the experiment. This fatigue test was chosen because it does not cause failure of neuromuscular transmission (4). All experiments were carried out in air-conditioned laboratories (20°C). With the use of a rectal thermometer (thermocouple), the body temperatures of the anaesthetized mice were monitored and varied between 30 and 33°C.

$[Ca^{2+}]_i$ measurements. Methods for enzymatic dissociation, agarose suspension, and loading of indo 1-AM into extensor digitorum longus (EDL) fibers and flexor digitorum brevis (FDB) fibers isolated from PV −/− and WT animals were the same as described previously (31), and $[Ca^{2+}]_i$-measurements were carried out at room temperature. Fibers were stimulated by a train of 3-ms pulses (separated by a 7-ms rest interval) for a total of 20- and 50-ms stimulation durations from a programmable voltage source via platinum wires. Indo 1 was excited with an ultraviolet laser source, and indo 1 fluorescence emission signals at 405 and 490 nm were collected by photomultiplier tubes, as described previously, using a Leica confocal setup with a fast line scan mode (13 ms/point) (31). The ratio (R) of the indo 1 emission signals (F_{405}/F_{490}) was used to calculate the $[Ca^{2+}]_i$ transients, as described previously, for fura 2 (8) using the following equation

$$[Ca^{2+}] = [dR/dt + k_{off}(R - R_{min})]/k_{on}(R_{max} - R) \quad (1)$$

The rate constants for binding (k_{on}) and dissociation (k_{off}) between Ca^{2+} and indo 1 have been determined by Westerblad and Allen (36) in *Xenopus* fibers. R_{max} was determined from long stimulation durations (50–200 ms), which clearly saturated the indicator with Ca^{2+}, and R_{min} was estimated by subtracting 15% of the mean resting ratio value. During the stimulation period (t = 100–300 ms) when the slow dissociation of Ca^{2+} from indo 1 would distort the Ca^{2+} transient, the derivative (dR/dt) was calculated for each individual point of the fluorescence ratio using the following equation

$$[R(n) - R(n-1)]/[t(n) - t(n-1)] \quad (2)$$

Before stimulation and after stimulation when indo 1 is expected to be in more equilibrium with Ca^{2+}, the derivative value was set to zero. A "bracket" pulse of two or more pulses was applied after the last pulse train of the experiment to insure that the fiber remained viable throughout the experiment and had not run down. All fibers included in this analysis exhibited a bracket ratio record that was at least 94% the amplitude of the first ratio record. $[Ca^{2+}]_i$ elevation (Ca^{2+}_{elev}) values were calculated using the following equation

$$Ca^{2+}_{elev} = Ca^{2+}_{post} - Ca^{2+}_{pre} \quad (3)$$

where the Ca^{2+} concentration after stimulation (Ca^{2+}_{post}) was determined by fitting a constant function from 200 to 700 ms after stimulation and Ca^{2+}_{pre} was the basal value, determined from a constant function fit of the first 100 ms before stimulation.

ELISA. The sandwich ELISA for PV is very similar to the one published in detail for calretinin (30). ELISA plates were pretreated with the monoclonal mouse anti-PV antibody PV235 (0.2 mg/ml in bidistilled water, diluted 1:50 in 100 mM $NaHCO_3$, pH 8.0; Swant, Bellinzona, Switzerland) for 16–24 h at room temperature. After two washes with water, the additional protein binding sites were blocked with 200 μl of 0.3 M Tris/acetate (pH 7.5) containing 1% BSA and 0.02% Kathon (Christ Chemie, Aesch, Switzerland) for 24 h. Standard curves (0–5 ng/ml of PV) were established with purified recombinant PV (Swant; 1 μg/ml of PV in a solution that contained 0.1 M Tris·HCl buffer, pH 6.5, 0.5% BSA, and 0.02% Kathon) and diluted in *buffer A* (0.3 M sodium acetate, pH 7.5, containing 10% FCS, 0.1% phenol, and 0.04% Kathon). For the isolation of soluble proteins, dissected muscles were homogenized in buffer (10 mM Tris and 2 mM EDTA, pH 7.5, containing a protease inhibitor cocktail from Roche, Mannheim, Germany) using a Polytron homogenizer (Kinematica, Luzern, Switzerland). The suspension was centrifuged (18,000 *g*, 4°C, 30 min), and the supernatant was used for ELISA. Protein concentrations were determined by the method of Bradford using reagents from Bio-Rad. Muscle extracts containing soluble proteins were diluted in the same solution as the purified PV and added together with the detection antibody rabbit anti-PV antiserum PV28 (Swant), diluted 1:800 with *buffer A*. After incubation of the samples for 24 h at room temperature, wells were washed twice with 0.05% (vol/vol) Tween 20 and twice with water. A peroxidase-

conjugated goat anti-rabbit IgG (Sigma, Buchs, Switzerland; 1:500 in *buffer A*) was added to each well and incubated for 2 h at room temperature, followed by washing four times with water. To detect the bound peroxidase, 200 μl of a 3,3′,5,5′-tetramethylbenzidine (TMB)-hydrogen peroxide solution (20 mM TMB and 50 mM hydrogen peroxide in acetone/ethanol; 10:90) was added to each well, and the development of the blue reaction product was blocked after 10–30 min by adding 100 μl of 1 M sulfuric acid. Absorbance was measured photometrically at 450 nm.

Morphometric analysis of mitochondrial fractional volume and capillaries in muscles from PV-deficient mice. For stereological analysis, dissected muscles [EDL and soleus (SOL)] were fixed in a solution of 80 mM sodium cacodylate, pH 7.3, containing 2% (wt/vol) paraformaldehyde, 2.5% (vol/vol) glutaraldehyde, and 0.2 mM $CaCl_2$, and was embedded in epon. Mitochondrial volume density of two different muscles (EDL and SOL) from three different animals per genotype was measured and statistically compared. Four tissue blocks per muscle were sectioned for electron microscopy. The orientation of the sections was transverse or slightly oblique with regard to the fiber axis. The volumes of mitochondria, myofibrils, and residual sarcoplasmic components per unit volume of muscle fiber were estimated on high-power electron micrographs at a final magnification of ×24,000. Systematic sampling with a random starting point was done in consecutive frames of 200 square mesh grids. Ten micrographs per section from all four blocks per muscle were taken and analyzed by point counting with grid C (144 test points). A second set of micrographs recorded at a final magnification of ×1,900 was used for estimation of capillary density and capillary-to-fiber ratio. Four micrographs per section were taken in consecutive frames of slotted grids. Point counting was done on the test system A 100 (100 test points). All stereological variables were calculated by applying standard procedures (35) as previously established (15).

$^{45}Ca^{2+}$ overlay blot of soluble proteins extracted from TA, EDL, and SOL. Adult mice (PV −/− and WT) were anaesthetized by inhalation of carbon dioxide and briefly perfused by ice-cold phosphate-buffered saline solution. After decapitation, the TA, EDL, and SOL muscles were excised. Muscles were homogenized in homogenization buffer (10 mM Tris·HCl and 1 mM EDTA, pH 7.4) using a Polytron homogenizer (Kinematica), and two different fractions, soluble and insoluble particulate, were prepared by centrifugation (30,000 *g* for 40 min).

Expression patterns of Ca^{2+}-binding proteins (including EF hand CaBP) were investigated by the Ca^{2+} overlay technique according to Maruyama et al. (24). Soluble proteins were separated by one-dimensional polyacrylamide gel electrophoresis (SDS-PAGE) on 12.5% polyacrylamide and then transferred onto a nitrocellulose membrane using a semi-dry transfer protocol. After transfer, membranes were washed three times for 20 min in freshly prepared solution (10 mM imidazole-HCl, 5 mM $MgCl_2$, and 60 mM KCl, pH 6.8) and then incubated for 10 min in solution that contained 40 kBq/ml of $^{45}CaCl_2$. Finally, membranes were washed for 5 min in 50% ethanol, dried, and exposed to a Molecular Imager screen for 24 h. The bands corresponding to the EF hand CaBPs with bound $^{45}Ca^{2+}$ were visualized by a Molecular Imager system (Bio-Rad).

Quantitative measurement of cytochrome c oxidase subunit I by Western blot analysis. The insoluble membrane protein/cytoskeleton fractions, isolated from both TA and EDL, were dissolved in 5% SDS, clarified by centrifugation, and protein concentrations in supernatants were determined by D_C protein assay (Bio-Rad) using the protocol supplied by the manufacturer. After dilution with 6× Laemmli sample buffer, 25 μg of proteins were separated by SDS-PAGE on a 10% polyacrylamide gel and transferred on nitrocellulose membranes using the semi-dry transfer protocol. Cytochrome *c* oxidase subunit I was detected using mouse monoclonal antibodies (clone 1D6-E1-A8) against human cytochrome *c* oxidase (Molecular Probes, Eugene, OR; A-6403) using the protocol according to Capaldi et al. (5) with slight modifications. Membranes were first blocked for 60 min at room temperature with 10% nonfat milk in TBS-T (10 mM Tris·HCl, pH 7.4, 500 mM NaCl, and 0.05% Tween 20) and then processed by the avidin-biotin blocking method using the manufacturer's protocol (Vector, Burlingame, CA). Incubation with primary antibodies (1 μg/ml, diluted in 0.1% BSA in TBS-T) and with biotinylated horse anti-mouse antibodies (Vector; diluted 1:10,000 in TBS-T) was 90 min at room temperature for both steps. The membrane was then incubated with peroxidase complex solution (Vectastain ABC kit; Vector) in TBS-T for 30 min, followed by extensive washing. Membranes were preincubated with enhanced chemiluminescence solution (Pierce, Rockford, IL) for 2 min and exposed for 5 min to a chemiluminescent screen (Bio-Rad). The bands corresponding to the cytochrome *c* oxidase subunit I were visualized and quantified using Molecular Imager hardware and software from the same manufacturer.

Statistical analysis. For all morphometric and force measurements and for the quantification of cytochrome *c* oxidase, values from PV +/− and PV −/− mice were compared with WT mice using the Student's *t*-test (unpaired, two-tailed). The values are expressed as means ± SD. Differences were considered significant at $P < 0.05$.

RESULTS

Increased resistance to muscle fatigue in fast-twitch muscles of PV knockout mice. We previously demonstrated that compared with muscles from WT mice, twitch duration is prolonged in fast-twitch muscles of PV −/− mice, while tension during maximal tetanic contraction is unaltered (31). Here, we have investigated the effects of PV deficiency on muscle fatigue. For this purpose, TA muscles were subjected to trains of tetanic contractions (40 Hz) of 250-ms durations every second for 5 min. This stimulation does not produce maximum force. Traces recorded from the three genotypes are shown in Fig. 1. A fatigue index was calculated as described in MATERIALS AND METHODS. The values were 0.32 ± 0.03 for WT ($n = 10$) and 0.44 ± 0.019 ($n = 6$) for PV −/−. Thus the PV-deficient muscles were significantly more resistant to fatigue than the WT muscles. However, the fatigue index of PV +/− mice was 0.228 ± 0.029 ($n = 6$), which showed them to be more fatigable then those from either PV −/− or WT mice. Factor(s) that may explain this difference in fatigability were studied next.

Basal $[Ca^{2+}]_i$ is not affected in PV knockout fast-twitch muscles, but kinetics of Ca^{2+} transients and Ca^{2+} clearance are altered. Consistent with our previous report, where we demonstrated that the resting $[Ca^{2+}]_i$ level in the PV −/− fast-twitch muscle EDL was not significantly different from the WT one [209 ± 66 nM vs. 117 ± 44 nM, respectively (31)], the FDB fibers analyzed in this study also showed no significant differences (190 ± 48 nM vs. 189 ± 49 nM in WT). On

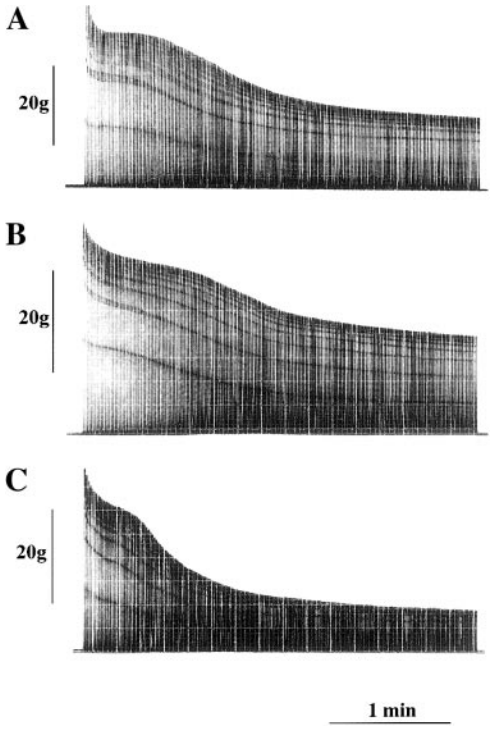

Fig. 1. Records of contractions elicited from the tibialis anterior (TA) muscles by repeated stimulation of the motor nerve at 40 Hz for 250 ms every second from a wild type (WT; *A*), a parvalbumin-deficient (PV −/−; *B*), and a heterozygous (PV +/−; *C*) mouse. A fatigue index was calculated from these recordings by dividing the force produced by the muscle at the end of the stimulation (5 min) by the force produced at the beginning of the experiment.

the other hand, the rate constant of $[Ca^{2+}]_i$ decay after 20 ms of stimulation was significantly decreased ($P < 0.05$) in mice lacking PV compared with WT animals in both EDL (31) and FDB fibers (183 + 29 s^{-1} in WT vs. 76 + 23 s^{-1} in PV −/−). Close analysis of the previous data on EDL fibers (31) and current data on FDB fibers revealed that not only the initial phase of decay of $[Ca^{2+}]_i$ was affected in PV −/−, but the kinetics of Ca^{2+} transients at later times were altered. As demonstrated in inhibitory PV-expressing hippocampal neurons (21) or in PV-loaded chromaffin cells (22), the kinetics of $[Ca^{2+}]_i$ decay in the presence of PV is biphasic. PV initially increases the rate of Ca^{2+} decay but then prolongs the transients by the release of Ca^{2+} from PV. In this study, the difference in $[Ca^{2+}]_i$ levels maintained from 200 to 700 ms after stimulation compared with the basal $[Ca^{2+}]_i$ maintained ~100 ms before stimulation was analyzed in both EDL and FDB fibers (Fig. 2). In WT mice, the net elevation of Ca^{2+} (mean of $Ca^{2+}_{elev} = \Delta[Ca^{2+}]_i$) was 10 nM for both EDL and FDB after 20 ms of stimulation (Fig. 2, *B* and *C*, respectively, open bars). Values were even higher after 50 ms of stimulation, 15 and 20 nM for EDL and FDB, respectively (Fig. 2, *B* and *C*, open bars), and reflect the higher degree of saturation of PV and thus an increased release of Ca^{2+} at the later phase of the transient. Interestingly, the degree of Ca^{2+} elevation was similar to levels of elevation observed in fast-twitch frog fibers stimulated for different durations (19). The amount of PV detected in PV +/− fibers of EDL and TA was between 40 and 50%, compared with WT (see below). Therefore, we hypothesized that the Ca^{2+} elevation due to Ca^{2+} release from PV should be smaller in PV +/− fibers 200 ms after stimulation compared with WT muscles. In both FDB and EDL fibers, $\Delta[Ca^{2+}]$ values were clearly smaller in PV +/− fibers stimulated for 20 or 50 ms (Fig. 2, *B* and *C*, hatched bars). This effect is not due to a reduced release of Ca^{2+} in PV +/− or PV −/− fibers, because we have shown previously that Ca^{2+} release in EDL fibers is not different among the three genotypes, and the time integral of the Ca^{2+} transient is actually slightly higher in PV +/− and PV −/− fibers (31). The results obtained on FDB fibers in this study were consistent with the previous findings, especially regarding the increased time integral of the Ca^{2+} transient determined in PV −/− fibers. Thus $\Delta[Ca^{2+}]$ values for PV −/− fibers were expected to be zero in PV −/− due to the complete lack of the slow Ca^{2+} buffer PV contributing to the Ca^{2+} elevation. However, in PV −/− FDB and EDL fibers, $[Ca^{2+}]_i$ 200 ms after stimulation was lower than before stimulation, resulting in negative $\Delta[Ca^{2+}]$ values of −40 nM in FDB at 50 ms of stimulation (Fig. 2*C*, filled bars). Although these values for FDB at 20 ms of stimulation and EDL (20 and 50 ms) also changed in the same direction ($\Delta[Ca^{2+}] < 0$), they did not reach statistical significance. These data suggested that system(s) contributing to Ca^{2+} clearance were more efficient or upregulated in fast-twitch muscles of PV −/− mice. The main mechanism for Ca^{2+} extrusion is the SR Ca^{2+}-ATPase, the activity of which differs between fast- and slow-twitch muscles (12). However, this activity was found not to be different between WT and PV −/− mice in four fast-twitch muscles (TA, EDL, psoas, and gastrocnemius) (28), and thus other systems implicated in Ca^{2+} clearance were investigated.

Cytosolic Ca^{2+}-binding proteins and proteins of the contractile complex are not altered in fast-twitch muscles of PV-deficient mice. Another possibility leading to the observed effects would be an upregulation of a soluble Ca^{2+} buffer protein similar to PV with a higher dissociation constant and even slower binding kinetics than PV. To test this possibility, total soluble protein extracts from TA, EDL, and the slow-twitch muscle SOL were isolated and analyzed by $^{45}Ca^{2+}$ overlay blots. The major band in WT muscles is PV (Fig. 3), which is clearly reduced in PV +/− and absent in PV −/− muscles. The amounts of PV were additionally quantified by ELISA and are in good agreement with the qualitative aspects of the $^{45}Ca^{2+}$ overlay blots (Table 1). In SOL muscle, the signals for PV are much weaker, because the PV content of type IIa fibers, which make up ~50% of total fibers, is very low, but the relative proportions in the three genotypes are maintained. The amount of PV in the three analyzed muscles (TA, EDL, and SOL; 2 mice/genotype) of heterozygous (PV +/−) mice is ~40–50% compared with WT animals (Table 1). A weaker band at ~20 kDa, most likely representing the ubiquitous Ca^{2+}-binding

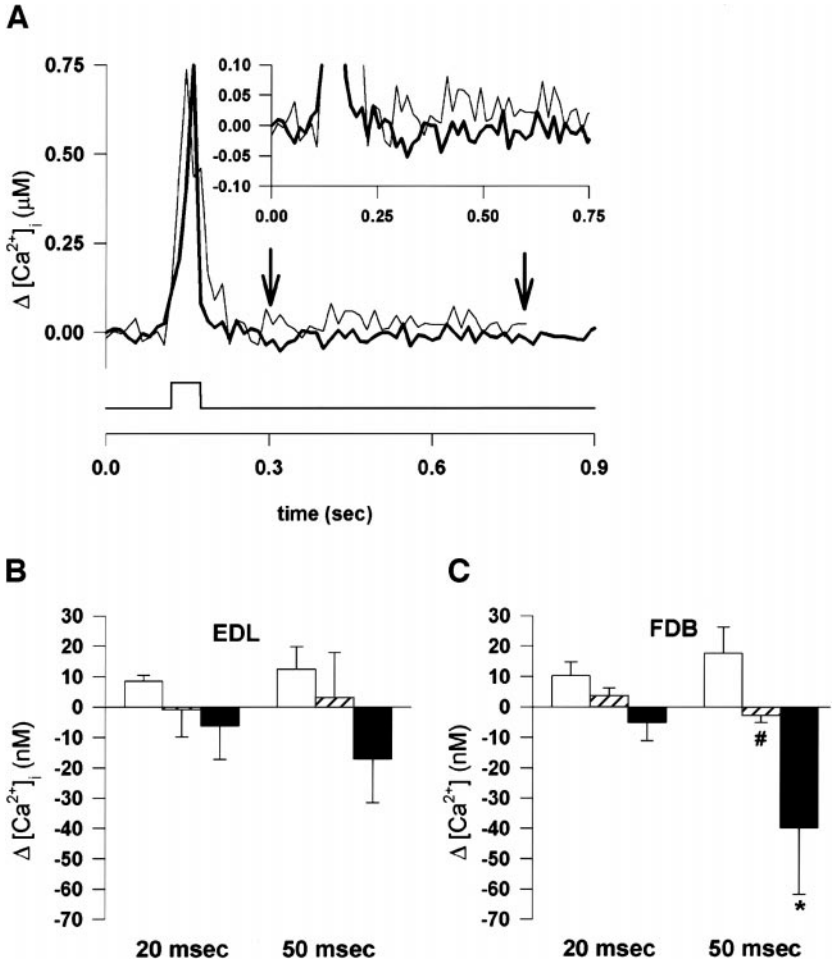

Fig. 2. Ca^{2+} transients in PV −/− and WT mice. *A*: 4 Ca^{2+} transients recorded from 50-ms stimulation durations were averaged for both WT (thin line) and PV −/− (thick line) flexor digitorum brevis (FDB) fibers and fit with a constant function from 200 to 700 ms after stimulation (time = 0.3 and 0.8 s, respectively, see arrows). Stimulation protocol is shown in the lower graph. To reveal differences in intracellular Ca^{2+} concentration ($[Ca^{2+}]_i$), following the initial decay more clearly, the axis has been changed in the *inset*. Ca^{2+} levels were determined 200 ms after stimulation (*A*) for all Ca^{2+} transients recorded from all 3 genotypes of extensor digitorum longus (EDL; *B*) and FDB (*C*) fibers. The mean differences ($\Delta[Ca^{2+}]_i$) in WT (open bars), PV +/− (hatched bars), and PV −/− (filled bars) fibers for 20 and 50 ms demonstrate that significant differences were observed between WT and PV −/− FDB fibers after a 50-ms stimulation duration (*WT vs. PV −/−, $P < 0.05$; #WT vs. PV +/−, $P < 0.05$). The differences between WT and PV −/− were not significant for EDL for 50 ms ($P = 0.087$) and FDB for 20 ms ($P = 0.066$) stimulation. The number (n) of fibers tested for EDL of WT, PV +/−, and PV −/− mice was 5, 6, and 4, respectively, and for FDB of WT, PV +/−, and PV −/− animals was 8, 8, and 5, respectively.

protein calmodulin (CaM), was observed in practically all samples, but considerable variations of signal intensities were observed between membranes. No other band representing a CaBP was detected in PV −/− muscles. Previously, we have shown that, in addition, all the other proteins of the contractile machinery [MHC isoforms (28) and troponins C, T, and I (31)] were not affected in fast-twitch muscles of PV −/− mice.

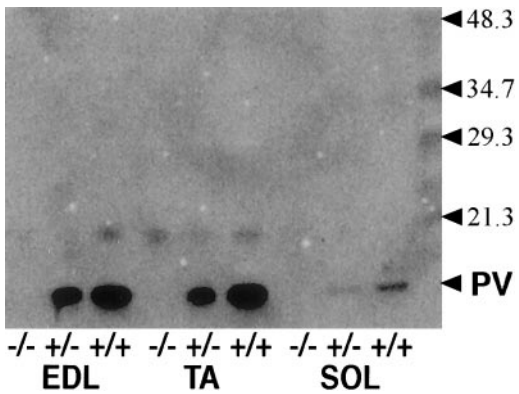

Fig. 3. $^{45}Ca^{2+}$ overlay blot of soluble proteins from TA, EDL, and soleus (SOL). Soluble proteins isolated from TA, EDL, and SOL of 3 genotypes were heated in the presence of 1 mM $CaCl_2$ at 60°C for 3 min. Thermal stable proteins (50 μg SOL, 40 μg TA, and 25 μg EDL) were separated by SDS-PAGE, transferred onto a nitrocellulose membrane, and incubated with a solution of $^{45}CaCl_2$. The most intense single band corresponds to PV. The positions of corresponding molecular weight standards are indicated by arrowheads.

Increased mitochondrial fractional volume and increased capillarization in fast-twitch muscle of PV −/− mice: link to fatigue resistance? In recent years, the role of mitochondria as a Ca^{2+} buffer or store has often been investigated, but the physiological relevance is still under debate. The fractional volume of mitochondria was determined by stereological analysis

Table 1. *Parvalbumin ELISA: soluble muscle protein*

Genotype	Muscle Type		
	TA, μg/mg	EDL, μg/mg	SOL, μg/mg
PV +/+	37.5	27.6	0.87
PV +/−	19.5	12.7	0.33
PV −/−	n.d.	n.d.	n.d.
%PV in +/− compared with WT	52 ± 2	46 ± 6	38 ± 5

Values are means ± SD with an average of 2 animals/genotype; n.d., not detectable (PV < 0.025 μg/mg of soluble muscle protein). TA, tibialis anterior; EDL, extensor digitorum longus; SOL, soleus; WT, wild type; PV, parvalbumin; PV −/−, PV deficient; PV +/−, heterozygous; PV +/+, wild type.

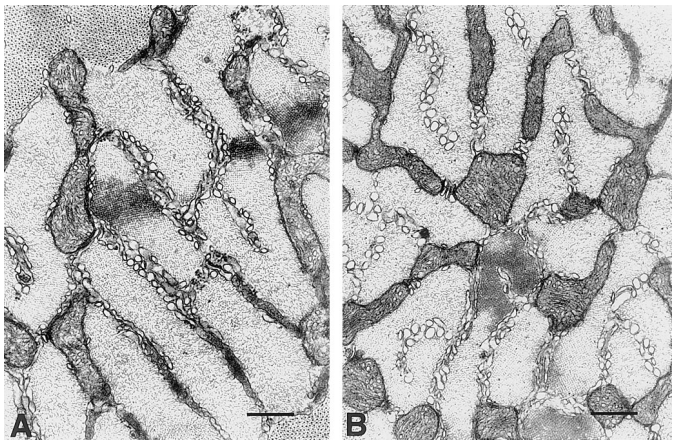

Fig. 4. Electron micrographs of cross-sectioned EDL myofibrils from a wild-type (*A*) and a PV-deficient (*B*) mouse. Scale bar: 0.5 μm.

in EDL and SOL of PV −/− and WT mice. The quality of the fixed tissue used for the evaluation is shown in Fig. 4 and demonstrates the integrity of the cellular structures including mitochondria. In EDL, the fractional volume was almost doubled in PV −/− (15.66 ± 0.54%) compared with WT (8.46 ± 0.61%) but only slightly (20%) increased in PV +/− (Table 2). A smaller increase (39 and 14%) was also detected in SOL of PV −/− and PV +/− mice, respectively. Using a biochemical assay, cytochrome *c* oxidase as a mitochondrial marker was determined by quantitative Western blot analysis. Its higher levels in samples from PV −/− were consistent with the results obtained by stereological analysis (Table 3). Cytochrome *c* oxidase in muscles from PV −/− mice was higher by ~55 and 38% in TA and EDL, respectively (Table 3). Interestingly, the number of capillaries per mm^2 surface [N_A(c,f)] was significantly higher (64% increase) in EDL of PV −/−, while values in WT and PV +/− mice were similar (Table 4). On the other hand, the average surface area of an EDL fiber was larger in PV +/− animals (1,638 ± 191 μm^2) compared with both other genotypes, 1,199 ± 197 μm^2 and 1,229 ± 125 μm^2 for PV +/+ and PV −/−, respectively. The increase in the density of capillaries (64%) in PV −/− EDL fibers paralleled the values determined for the mitochondria parameters (85% in PV −/− EDL fibers, Table 2). Thus it is evident that both mitochondrial volumes and capillary densities are higher in PV −/− mice, and this is most prominent in fast-twitch muscles lacking PV.

Table 2. *Total mitochondrial volumes in EDL and SOL in PV-deficient, heterozygous, or wild-type mice*

	PV +/+	PV +/−	PV −/−
EDL			
%V_V(mt,f),	8.46 ± 0.61	10.38 ± 0.25	15.66 ± 0.54*
%control	100 ± 7†	123 ± 2	185 ± 3
SOL			
%V_V(mt,f),	15.42 ± 1.35	17.54 ± 1.66	21.49 ± 1.54*
%control	100 ± 9†	114 ± 3	139 ± 7

Values are means ± SD. *Student's *t*-test (unpaired) in EDL (PV +/+ vs. PV −/−, $P < 0.001$) and in SOL (PV +/+ vs. PV −/−, $P < 0.01$). †The value for PV +/+ was set at 100%. %V_V(mt,f), total mitochondrial volume.

Table 3. *Mitochondria parameters: cytochrome c oxidase*

	Genotype	
Muscle Type	PV +/+	PV −/−
TA arbitrary units	121.1 ± 24.1	187.8 ± 32.6
%Control	100 ± 19.9	155 ± 26.9*
EDL arbitrary units	45.6 ± 7.03	63.1 ± 4.06
%Control	100 ± 15.4	138 ± 8.9†

Values are means ± SD. Relative levels compared with PV +/+ (=100%) in TA and EDL of PV −/− mice. *Student's *t*-test (unpaired), $P < 0.001$; †Student's *t*-test (unpaired), $P < 0.05$.

DISCUSSION

Ca^{2+} plays a crucial role as a second messenger in many biological processes, including gene regulation. Its role is exerted either indirectly via Ca^{2+}/CaM-dependant pathways (e.g., CaM kinases leading to the phosphorylation of cAMP-responsive element binding protein) (2, 13) or it can act directly with specific Ca^{2+}-dependant transcriptional proteins, such as DREAM, which represses transcription from the early response gene c-*fos* (6). Ca^{2+}-induced alterations in gene expression are also observed in skeletal myofibers. Application of Ca^{2+} ionophore to cultured myotubes, which develop the adult pattern of fast myosin light and heavy chains, alters the expression pattern toward slow isoforms. This process is paralleled by an increase of the citrate synthase activity and is reversible after withdrawal of the ionophore (20). Cytochrome *c* expression was also shown to be upregulated in myotubes after ionophore treatment (10). However, these experimental models do not reflect the physiological situation, because the increase in $[Ca^{2+}]_i$ is permanent, whereas during activity, the changes of $[Ca^{2+}]_i$ are transient and the amplitude as well as the spatial and temporal distribution of these transients may determine which pathways are activated. Thus specific information is contained in the amplitude as well as the frequency of Ca^{2+} signals (1), and highly specialized systems for Ca^{2+} release, intracellular buffering, and Ca^{2+} extrusion determine the shape of the transients. In the myoplasm, the frequency, magnitude, and kinetics of elevations and decay of $[Ca^{2+}]_i$ depend on the frequency of stimulation by the motor neuron, the kinetics of release from the SR, soluble Ca^{2+} buffers, and the Ca^{2+} uptake system, including SR and mitochondria. In fast-twitch muscles of PV-deficient mice, Ca^{2+} transients induced by electrical stimulation of isolated EDL fibers have the same rate of rise and peak amplitude, which is reflected by the unchanged kinetics of contraction during the initial phase (31). This indicates that systems that contribute to the rise of $[Ca^{2+}]_i$ are not affected by the lack of PV. On the other hand, the initial rate of $[Ca^{2+}]_i$ decay is significantly lower compared with WT fibers (31) and is consistent with results obtained either on inhibitory

Table 4. *Muscle fiber parameters related to vascularization*

Muscle		Genotype			PV+/+ vs. PV−/− PV+/+ vs. PV+/−
		PV +/+	PV +/−	PV −/−	
EDL	N_A(c,f)	$890 \pm 40\,mm^{-2}$	$911 \pm 36\,mm^{-2}$	$1,464 \pm 72\,mm^{-2}$	$P < 0.001$
	%control	100 ± 4	102 ± 4	164 ± 8	n.s.
	a (f)	$1,199 \pm 197\,\mu m^2$	$1,638 \pm 191\,\mu m^2$	$1,229 \pm 125\,\mu m^2$	n.s.
	%control	100 ± 16	137 ± 16	103 ± 10	$P < 0.05$
SOL	N_A(c,f)	$1,043 \pm 243\,mm^{-2}$	$1,401 \pm 125\,mm^{-2}$	$1,758 \pm 154\,mm^{-2}$	$P < 0.02$
	%control	100 ± 23	134 ± 12	169 ± 15	n.s.
	a (f)	$1,957 \pm 507\,\mu m^2$	$1,722 \pm 105\,\mu m^2$	$1,649 \pm 238\,\mu m^2$	n.s.
	%control	100 ± 26	88 ± 5	84 ± 12	n.s.

Values are means ± SD. N_A(c,f), number of capillaries/mm² fiber surface; a (f), average surface per fiber (μm²); n.s., not significant.

hippocampal neurons (21) or PV-injected chromaffin cells (22) in which the rate of $[Ca^{2+}]_i$ decay was significantly increased by PV. In the late phase of $[Ca^{2+}]_i$ decay, however, PV is expected to prolong the transient due to the release of Ca^{2+} from PV (22). Analyses of the Ca^{2+} transients of EDL and FDB fibers from PV −/− mice show that although the initial decay of $[Ca^{2+}]_i$ is slower, this is followed by a period with even lower $[Ca^{2+}]_i$ than before the stimulation. This "negative elevation" was seen only in PV −/− fast-twitch muscles and was more prominent during stimulation of longer duration (50-ms vs. 20-ms stimulation), indicative of an additional or enhanced system of Ca^{2+} buffering or Ca^{2+} removal. In gel overlay assays, no evidence for upregulation of another Ca^{2+}-binding protein was obtained, especially not in the PV −/− mice. Only one relatively weak signal compared with PV (with a relative molecular mass ~20 kDa, most likely representing CaM) was observed, but it was not different in the three genotypes. Even if another as yet unidentified CaBP existed, the properties of this protein would have to include slower Ca^{2+}-binding kinetics than PV and no refolding of the Ca^{2+}-binding domains in the presence of Ca^{2+} on the nitrocellulose membranes, two characteristics that have not been observed in another EF hand CaBP. The activity of the SR Ca^{2+}-ATPase, the most effective system of Ca^{2+} reuptake in fast-twitch muscles, was unaffected in all investigated muscles of PV −/− mice when tested in vitro (28). However, it could be that the increase in oxidative enzymes seen in this study led to a faster rephosphorylation of ATP so that the ratio of ATP:ADP was higher and the phosphorylation potential greater. This would lead to a more efficient Ca^{2+} pump (38) and may account for the "overshoot" of Ca^{2+} removal that was particularly obvious after prolonged stimulation. Another possibility is that the increased number of mitochondria not only provides the higher levels of oxidative enzymes but also plays a direct role in Ca^{2+} sequestration. The possible role of mitochondria in Ca^{2+} sequestration during relaxation of slow-twitch and cardiac muscles has previously been discussed in detail by Lehninger (23). According to this author, the Ca^{2+} sequestration by mitochondria encompasses two separate processes. The process involved in fast Ca^{2+} sequestration most likely relates to its binding to the mitochondrial membrane ("membrane loading"), whereas "matrix loading" represents the slower component. The role of mitochondria in Ca^{2+} signaling, their role as a Ca^{2+} store or sink, and their involvement in muscle fatigue have gained much attention in recent years (9, 11, 32), and development of new techniques has allowed the investigation of the dynamics of mitochondrial Ca^{2+} ($[Ca^{2+}]_{mit}$) (29). Earlier experiments have demonstrated that $^{45}Ca^{2+}$ uptake is significantly faster in mitochondria from slow-twitch, oxidative fibers (STR), compared with fast-twitch, glycolytic fibers (32). It was hypothesized that mitochondrial Ca^{2+} uptake in STR could account for up to 100% contributing to the relaxation rate at low-frequency stimulation. Evidence for an involvement of mitochondria in the relaxation of slow-twitch fibers was provided by Gillis (11) using the mitochondrial Ca^{2+} uptake inhibitor ruthenium red. The rate of relaxation in the presence of the inhibitor was significantly decreased in slow-twitch muscles, while not affecting the contraction-relaxation cycle of fast-twitch muscles.

As demonstrated previously (31) and in this study either directly or indirectly, proteins of the contractile apparatus [MHC isoforms (28), troponins T and I], SR Ca^{2+}-ATPase activity, and Ca^{2+} release from the SR were not affected by the lack of PV. The present results show that in addition to the slower time course of contraction and relaxation, the only differences that were clearly detectable in PV −/− fast-twitch fibers were the increase in mitochondria (evidenced by the increased fractional volume and cytochrome *c* oxidase) and the increased capillarization. The changes of contractile properties are evident, because removal of Ca^{2+} by mitochondria sets in with a delay, thus the kinetics of a twitch in a PV −/− fast-twitch muscle is still slower than in a WT mouse, despite an almost doubling of mitochondrial fractional volume. On the other hand, the increases in mitochondria and capillarization provide the most likely explanation for the enhanced resistance of PV −/− fast-twitch muscles to fatigue. In PV +/− EDL fibers in which the PV content is ~50–60% smaller than in WT ones, the mitochondrial volume is only slightly elevated, the capillary density is similar to WT fibers, and the average fiber size is larger. Interestingly, these changes together result in a higher sensitivity to fatigue compared with WT muscles.

From our results, several concepts and hypotheses can be put forward. *1*) The alteration in the shape of a Ca^{2+} transient (slower Ca^{2+} decay) is sufficient to induce mitochondrial biogenesis and does not require sustained Ca^{2+} elevations. The mitochondrial volume in EDL of PV −/− mice (15.66 ± 0.54%) is similar to that found in the slow-twitch muscle SOL of WT animals (15.42 ± 1.35%). *2*) The increased volume of mitochondria in PV −/− is not sufficient to revert twitch parameters to those of the WT, due to the slow kinetics of Ca^{2+} uptake compared with PV. Thus mitochondria cannot accurately compensate for the deficiency of PV. Nevertheless, their increase in the fast muscles is most likely responsible for the change in the resistance to fatigue. Whether the altered Ca^{2+} transients are directly linked to enhanced capillarization or if the signal is transmitted through the increased mitochondrial volume remains to be investigated. Findings that increases in capillarization precede the increases in key enzymes of mitochondrial energy metabolism in low-frequency stimulated rabbit TA (3, 33) argue against the possibility that the increase in mitochondria is responsible for the growth of capillaries. In rats and rabbits, chronic low-frequency stimulation induces, in addition to the downregulation of PV and elevations in capillary and mitochondrial densities, fiber type transitions. These transitions encompass multiple exchanges of fast-type with slow-type isoforms of thick and thin filament proteins, as well as of the SR Ca^{2+}-ATPase and several other membrane proteins related to Ca^{2+} release and sequestration (26, 27). In the mouse, low-frequency electrical stimulation does not induce changes of fiber types, and this is consistent with the present finding on the lack of fiber type transitions in PV −/− mouse muscles. This makes it much easier to relate the observed changes in the physiological properties to the altered Ca^{2+} transients and the increase in mitochondrial density. *3*) The possibility exists that the transition of fast-twitch to the slow-twitch fiber isoforms (MHC, troponins, SR Ca^{2+}-ATPases) fails to occur in PV −/− mice because increases in mitochondria and oxidative capacity of the muscle fibers reduce $[Ca^{2+}]_i$ after the contraction. Thus the signal, i.e., prolonged increased levels of $[Ca^{2+}]_i$, is not maintained long enough to drive the system all the way toward a slow muscle fiber. The lack of isoform conversion of proteins involved in muscle contraction in mice after CLFS indicates that the relatively high content and rapid increase in mitochondria in this species may attenuate the signals involved in fiber type transitions.

We thank P. Nicotera, University of Konstanz, for use of the confocal imaging system. The excellent technical help of I. Marquardt (Konstanz), C. Pythoud and V. Neuhaus (Fribourg), and W. Graber (Bern) is greatly appreciated. H. Hoppeler's group was of great assistance in establishing the morphometric measurements. We are grateful to Drs. Merdol Ibrahim and Jean-Marie Gillis for critical reading of the manuscript.

The project was supported by Swiss National Science Foundation Grant 3100–047291.96 (to M. Celio) and Novartis.

REFERENCES

1. **Berridge MJ and Dupont G.** Spatial and temporal signalling by calcium. *Curr Opin Cell Biol* 6: 267–274, 1994.
2. **Bito H, Deisseroth K, and Tsien RW.** CREB phosphorylation and dephosphorylation: a Ca(2+)- and stimulus duration-dependent switch for hippocampal gene expression. *Cell* 87: 1203–1214, 1996.
3. **Brown MD, Cotter MA, Hudlicka O, and Vrbova G.** The effects of different patterns of muscle activity on capillary density, mechanical properties and structure of slow and fast rabbit muscles. *Pflügers Arch* 361: 241–250, 1976.
4. **Burke RE.** Motor units: Anatomy, physiology and functional organization, edited by Brooks VB. In: *Handbook of Physiology. The Nervous System. Motor Control.* Bethesda, MD: Am. Physiol. Soc., 1981, sect. 1, vol. II, pt. 1, p. 345–422.
5. **Capaldi RA, Marusich MF, and Taanman JW.** Mammalian cytochrome-*c* oxidase: characterization of enzyme and immunological detection of subunits in tissue extracts and whole cells. *Methods Enzymol* 260: 117–132, 1995.
6. **Carrion AM, Link WA, Ledo F, Mellstrom B, and Naranjo JR.** DREAM is a Ca^{2+}-regulated transcriptional repressor. *Nature* 398: 80–84, 1999.
7. **Carroll S, Nicotera P, and Pette D.** Calcium transients in single fibers of low-frequency stimulated fast-twitch muscle of rat. *Am J Physiol Cell Physiol* 277: C1122–C1129, 1999.
8. **Carroll SL, Klein MG, and Schneider MF.** Decay of calcium transients after electrical stimulation in rat fast- and slow-twitch muscle fibres. *J Physiol* 501: 573–588, 1997.
9. **Duchen MR.** Contributions of mitochondria to animal physiology: from homeostatic sensor to calcium signalling and cell death. *J Physiol (Lond)* 516: 1–17, 1999.
10. **Freyssenet D, Di Carlo M, and Hood DA.** Calcium-dependent regulation of cytochrome *c* gene expression in skeletal muscle cells. Identification of a protein kinase C-dependent pathway. *J Biol Chem* 274: 9305–9311, 1999.
11. **Gillis JM.** Inhibition of mitochondrial calcium uptake slows down relaxation in mitochondria-rich skeletal muscles. *J Muscle Res Cell Motil* 18: 473–483, 1997.
12. **Hämäläinen N and Pette D.** Coordinated fast-to-slow transitions of myosin and SERCA isoforms in chronically stimulated muscles of euthyroid and hyperthyroid rabbits. *J Muscle Res Cell Motil* 18: 545–554, 1997.
13. **Hardingham GE, Chawla S, Johnson CM, and Bading H.** Distinct functions of nuclear and cytoplasmic calcium in the control of gene expression. *Nature* 385: 260–265, 1997.
14. **Hicks A, Ohlendieck K, Gopel SO, and Pette D.** Early functional and biochemical adaptations to low-frequency stimulation of rabbit fast-twitch muscle. *Am J Physiol Cell Physiol* 273: C297–C305, 1997.
15. **Hoppeler H, Mathieu O, Krauer R, Claassen H, Armstrong RB, and Weibel ER.** Design of the mammalian respiratory system. VI. Distribution of mitochondria and capillaries in various muscles. *Respir Physiol* 44: 87–111, 1981.
16. **Huber B and Pette D.** Dynamics of parvalbumin expression in low-frequency-stimulated fast-twitch rat muscle. *Eur J Biochem* 236: 814–819, 1996.
17. **Hudlicka O, Brown M, Cotter M, Smith M, and Vrbova G.** The effect of long-term stimulation of fast muscles on their blood flow, metabolism and ability to withstand fatigue. *Pflügers Arch* 369: 141–149, 1977.
18. **Jiang Y, Johnson JD, and Rall JA.** Parvalbumin relaxes frog skeletal muscle when sarcoplasmic reticulum Ca^{2+}-ATPase is inhibited. *Am J Physiol Cell Physiol* 270: C411–C417, 1996.
19. **Klein MG, Simon BJ, Szucs G, and Schneider MF.** Simultaneous recording of calcium transients in skeletal muscle using high- and low-affinity calcium indicators. *Biophys J* 53: 971–988, 1988.
20. **Kubis HP, Haller EA, Wetzel P, and Gros G.** Adult fast myosin pattern and Ca^{2+}-induced slow myosin pattern in primary skeletal muscle culture. *Proc Natl Acad Sci USA* 94: 4205–4210, 1997.
21. **Lee SH, Rosenmund C, Schwaller B, and Neher E.** Differences in Ca^{2+} buffering properties between excitatory and inhib-

itory hippocampal neurons from the rat. *J Physiol (Lond)* 525: 405–418, 2000.
22. **Lee SH, Schwaller B, and Neher E.** Kinetics of Ca^{2+} binding to parvalbumin in bovine chromaffin cells: implications for $[Ca^{2+}]$ transients of neuronal dendrites. *J Physiol (Lond)* 525: 419–432, 2000.
23. **Lehninger AL.** Ca^{2+} transport by mitochondria and its possible role in the cardiac contraction-relaxation cycle. *Circ Res* 35, *Suppl* 3: 83–90, 1974.
24. **Maruyama K, Mikawa T, and Ebashi S.** Detection of calcium binding proteins by ^{45}Ca autoradiography on nitrocellulose membrane after sodium dodecyl sulfate gel electrophoresis. *J Biochem (Tokyo)* 95: 511–519, 1984.
25. **Muntener M, Kaser L, Weber J, and Berchtold MW.** Increase of skeletal muscle relaxation speed by direct injection of parvalbumin cDNA. *Proc Natl Acad Sci USA* 92: 6504–6508, 1995.
26. **Ohlendieck K, Fromming GR, Murray BE, Maguire PB, Leisner E, Traub I, and Pette D.** Effects of chronic low-frequency stimulation on Ca^{2+}-regulatory membrane proteins in rabbit fast muscle. *Pflügers Arch* 438: 700–708, 1999.
27. **Pette D and Vrbova G.** Adaptation of mammalian skeletal muscle fibres to chronic electrical stimulation. *Rev Physiol Biochem Pharmacol* 120: 116–202, 1992.
28. **Raymackers JM, Gailly P, Schoor MC, Pette D, Schwaller B, Hunziker W, Celio MR, and Gillis JM.** Tetanus relaxation of fast skeletal muscles of the mouse made parvalbumin deficient by gene inactivation. *J Physiol* 527: 355–364, 2000.
29. **Rizzuto R, Simpson AWM, Brini M, and Pozzan T.** Rapid changes of mitochondrial Ca^{2+} revealed by specifically targeted recombinant aequorin. *Nature* 358: 325–327, 1992.
30. **Schwaller B, Bruckner G, Celio MR, and Hartig W.** A polyclonal goat antiserum against the calcium-binding protein calretinin is a versatile tool for various immunochemical techniques. *J Neurosci Methods* 92: 137–144, 1999.
31. **Schwaller B, Dick J, Dhoot G, Carroll S, Vrbova G, Nicotera P, Pette D, Wyss A, Bluethmann H, Hunziker W, and Celio MR.** Prolonged contraction-relaxation cycle of fast-twitch muscles in parvalbumin knockout mice. *Am J Physiol Cell Physiol* 276: C395–C403, 1999.
32. **Sembrowich WL, Quintinskie JJ, and Li G.** Calcium uptake in mitochondria from different skeletal muscle types. *J Appl Physiol* 59: 137–141, 1985.
33. **Skorjanc D, Jaschinski F, Heine G, and Pette D.** Sequential increases in capillarization and mitochondrial enzymes in low-frequency-stimulated rabbit muscle. *Am J Physiol Cell Physiol* 274: C810–C818, 1998.
34. **Stephenson DG, Lamb GD, and Stephenson GMM.** Events of the excitation-contraction-relaxation (E-C-R) cycle in fast- and slow-twitch mammalian muscle fibres relevant to muscle fatigue. *Acta Physiol Scand* 162: 229–245, 1998.
35. **Weibel ER.** Stereological methods. In: *Practical Methods For Biological Morphometry*. New York: Academic, 1979.
36. **Westerblad H and Allen DG.** Intracellular calibration of the calcium indicator indo-1 in isolated fibres of *Xenopus* muscle. *Biophys J* 71: 908–917, 1996.
37. **Westerblad H and Allen DG.** Slowing of relaxation and $[Ca^{2+}]_i$ during prolonged tetanic stimulation of single fibres from *Xenopus* skeletal muscle. *J Physiol* 492: 723–736, 1996.
38. **Zweier JL, Jacobus WE, Korecky B, and Brandejs-Barry Y.** Bioenergetic consequences of cardiac phosphocreatine depletion induced by creatine analog feeding. *J Biol Chem* 266: 20296–20304, 1991.